in central and northern Europe. *Bulletin of the Geological Society of America*, **96**, 1554–1571.
Vandergoes, M. J., Hogg, A. G., Lowe, D. J., Newnham, R. M., Denton, G. H., Southon, J., Barrell, D. J. A., Blaauw, M., Wilson, C. J. N., McGlone, M. S., Allan, A. S. R., Almond, P. C., Petchey, F., Dalbell, K., and Dieffenbacher-Krall, A. C., 2013. A revised age for the Kawakawa/Oruanui tephra, a key marker for the Last Glacial Maximum in New Zealand. *Quaternary Science Reviews*, **74**, 195–200.
Westgate, J. A., 1989. Isothermal plateau fission track ages of hydrated glass shards from silicic tephra beds. *Earth and Planetary Science Letters*, **95**, 226–234.
Westgate, J. A., Smith, D. G. W., and Nichols, H., 1969. Late Quaternary pyroclastic layers in the Edmonton area, Alberta. In Pawluk, S. (ed.), *Pedology and Quaternary Research*. Edmonton: University of Alberta, pp. 179–186.
Westgate, J. A., Stemper, B. A., and Péwé, T. L., 1990. A 3 m.y. record of Pliocene-Pleistocene loess in interior Alaska. *Geology*, **18**, 858–861.
Westgate, J., Shane, P., Pearce, N., Perkins, W., Korisettar, R., Chesner, C. A., Williams, M., and Acharyya, S. K., 1998. All Toba tephra occurrences across Peninsular India belong to the 75,000 yr B.P. eruption. *Quaternary Research*, **50**, 107–112.
Westgate, J. A., Preece, S. J., Froese, D. G., Pearce, N. J. G., Roberts, R. G., Demuro, M., Hart, W. K., and Perkins, W., 2008. Changing ideas on the identity and stratigraphic significance of the Sheep Creek tephra beds in Alaska and the Yukon Territory, northwestern North America. *Quaternary International*, **178**, 183–209.
Westgate, J. A., Pearce, N. J. G., Perkins, W. T., Shane, P. A. R., and Preece, S. J., 2011. Lead isotope ratios of volcanic glass by laser ablation inductively-coupled plasma mass spectrometry: application to Miocene tephra beds in Montana, USA and adjacent areas. *Quaternary International*, **246**, 89–96.
Westgate, J. A., Pearce, G. W., Preece, S. J., Schweger, C. E., Morlan, R. E., Pearce, N. J. G., and Perkins, W. T., 2013a. Tephrochronology, magnetostratigraphy and mammalian faunas of Middle and Early Pleistocene sediments at two sites on the Old Crow River, northern Yukon Territory, Canada. *Quaternary Research*, **79**, 75–85.
Westgate, J. A., Naeser, N. D., and Alloway, B. V., 2013b. Fission-track dating. In Elias, S. A., and Mock, C. J. (eds.), *The Encyclopaedia of Quaternary Science*, 2nd edn. Amsterdam: Elsevier, Vol. 1, pp. 643–662.
Westgate, J. A., Pearce, N. J. G., Perkins, W. T., Preece, S. J., Chesner, C. A., and Muhammad, R. F., 2013c. Tephrochronology of the Toba tuffs: four primary glass populations define the 75 ka Youngest Toba Tuff, northern Sumatra, Indonesia. *Journal of Quaternary Science*, **28**, 772–776.
White, J. F. L., and Houghton, B. F., 2006. Primary volcaniclastic rocks. *Geology*, **34**, 677–680.
Wilson, C. J. N., Gravley, D. M., Leonard, G. S., and Rowland, J. V., 2009. Volcanism in the central Taupo Volcanic Zone, New Zealand: tempo, styles and controls. In Thordarson, T., Self, S., Larsen, G., Rowland, S. K., and Hoskuldsson, A. (eds.), *Studies in Volcanology: The Legacy of George Walker*. London: Geological Society. Special publications of IAVCEI, Vol. 2, pp. 225–247.
Wilson, C. J. N., Charlier, B. L. A., Rowland, J. V., and Browne, P. R. L., 2010. U-Pb dating of zircon in subsurface, hydrothermally altered pyroclastic deposits and implications for subsidence in a magmatically active rift: Taupo Volcanic Zone, New Zealand. *Journal of Volcanology and Geothermal Research*, **191**, 69–78.
Yin, J., Jull, A. J. T., Burr, G. S., and Zheng, Y., 2012. A wiggle-match age for the Millennium eruption of Tianchi Volcano at Changbaishan, northeastern China. *Quaternary Science Reviews*, **47**, 150–159.
Zalasiewicz, J., Cita, M. B., Hilgen, F., Pratt, B. R., Strasser, A., Thierry, J., and Weissert, H., 2013. Chronostratigraphy and geochronology: a proposed realignment. *GSA Today*, **23**, 4–8.
Zdanowicz, C. M., Zielinski, G. A., and Germani, M. S., 1999. Mount Mazama eruption: calendrical age verified and atmospheric impact assessed. *Geology*, **27**, 621–624.

Cross-references

Accelerator Mass Spectrometry
Ar–Ar and K–Ar Dating
Biostratigraphy
^{14}C in Plant Macrofossils
Dendrochronology, Volcanic Eruptions
Fission Track Dating and Thermochronology
Ice Cores
Laser Ablation Inductively Coupled Mass Spectrometer (LA ICP-MS)
Lacustrine Environments (^{14}C)
Luminescence Dating
Magnetostratigraphic Dating
Marine Isotope Stratigraphy
Paleosol
^{210}Pb Dating
Peat (^{14}C)
Radiocarbon Dating
Sedimentary Rocks (Rb-Sr Geochronology)
Single-Crystal Laser Fusion
Uranium–Lead, Zircon
U–Th/He Dating
Volcanic Glass (Fission Track)
Zircon

TERRESTRIAL COSMOGENIC NUCLIDE DATING

John Gosse[1] and Jeff Klein[2]
[1]Department of Earth Sciences, Dalhousie University, Halifax, NS, Canada
[2]Department of Physics and Astronomy, University of Pennsylvania, Philadelphia, PA, USA

Synonyms

Burial dating; Cosmic ray exposure (CRE) dating; Cosmogenic nuclide isochron dating; Cosmogenic radionuclide (CRN) dating; Depth profile dating; Surface exposure dating (SED); Terrestrial in situ cosmogenic nuclide (TCN) exposure histories

Definitions

Cosmic rays are high-energy (10^4 to 10^{20} eV) particles composed mostly (90 %) of atomic nuclei but with some photons (gamma rays), electrons, and positrons. The majority (90 %) of the atomic nuclei are protons (H nuclei), the rest are alpha particles (He nuclei, 9 %) and nuclei heavier atoms (1 %). Two major sources of this *primary cosmic radiation* are the Sun whose flux peaks at ~100 MeV (solar cosmic rays, *SCR*) and our galaxy,

the Milky Way, with the flux peak between 300 MeV and 1 Gev (galactic cosmic rays, *GCR*). We believe GCR is produced primarily in supernova events (an inference suggested by the excess over cosmic abundance of heavy nuclei).

Secondary cosmic radiation (or "secondaries") refers to the cascade of particles produced by the interaction of primary cosmic rays with the atmosphere and the surface of the Earth. Because of the high energies of the incoming particles, a wide spectrum of hadrons, mesons, and leptons are produced. The lifetimes of many of these secondary particles are so short that they decay in a shower of lighter particles before they can interact with another atom of the material through which they are passing, but others do interact, producing yet another cascade. Ultimately, the flux is dominated by the longer-lived particles and by the particles with small interaction cross sections. By the time the primaries have passed through 10 % of the atmosphere, the secondary flux is predominately pions, kaons, protons, neutrons, muons, electrons, positrons, and gamma rays (photons). These secondaries will produce larger nuclei (cosmogenic nuclides) in the atmosphere and minerals.

Cosmogenic nuclides are produced through any interaction of primary or secondary cosmic radiation with matter. While some notable cosmogenic nuclides (isotopes) are produced from SCR (e.g., atmospheric radiocarbon is produced from low-energy (thermal) *neutron capture* by nitrogen: $^{14}N(n, p)^{14}C$), the majority of TCN production is through *spallation* of a target nucleus which requires GCR primaries or secondaries with sufficient energy to exceed the binding energy of the target nucleus (a minimum of >3 MeV per target nucleon). Cosmogenic nuclides need to be distinguished from radiogenic and nucleogenic nuclides. A *radiogenic nuclide* is a daughter product of a radioactive decay (fission, beta, alpha). For U-dating methods or (U–Th)/He thermochronology, $^{234}Th + {}^{4}He$ are radiogenic products of the α-decay of ^{238}U. A *nucleogenic nuclide* is produced when an energetic radiogenic particle interacts with another nucleus just after decay of its parent. For example, ^{10}Be can be produced in a lithium-rich mineral via $^{7}Li(\alpha, p)^{10}Be$.

Cosmogenic nuclide dating uses the accumulation, production, or decay of cosmogenic nuclides to determine the exposure history of near-surface samples (top tens of meters on Earth or top hundreds of meters in space). This can be accomplished by measuring a cosmogenic isotope that has been produced in situ in a mineral on a rock surface or that has been produced in the atmosphere and subsequently accumulated in a soil. For instance, the concentration of ^{10}Be accumulated in a saprolite will depend on the flux of ^{10}Be in precipitation and dust delivered to the soil, the abundance and type of clay that holds the ^{10}Be, and the duration that the soil is at the surface. In addition to exposure ages, the method can determine whether a sample was at the surface or beneath it, whether the sample's position was stable or eroding, and whether the sample's surface history was interrupted by periods of burial. Examples of applications of cosmogenic nuclides that are produced in situ, but not in Earth's lithosphere, include surface exposure dating on Martian (Farley et al., 2014) and lunar surfaces (Drozd et al., 1974) and the size and exposure history of meteorites (Eugster et al., 2006). Cosmogenic nuclides produced in the atmosphere include ^{14}C (thermal-neutron capture by N). Radiocarbon dating has been widely applied for dating objects of importance in defining geologic and archaeologic chronologies; in testing the authenticity of objects of art, or worship, or historic significance; and, on even shorter time scales, in studying the inception and progress of disease in a living organism. ^{14}C has been used to study atmospheric mixing, verify the global circulation model of the oceans, and follow the fate of anthropogenic carbon in the biosphere and oceans. ^{36}Cl produced in the atmosphere by cosmic ray-induced spallation of argon has been used primarily by hydrologists to study the recharge histories of hydrologic systems. ^{10}Be and ^{7}Be produced in the atmosphere have been used to estimate ages of soils and ground ice (e.g., Gilichinsky et al., 2007) or rates of erosion of catchments (Brown et al., 1988) and study the behavior of aerosol deposition and air mass mixing.

Broadly, there are three types of systems that are dated using cosmogenic nuclides: (1) those in which the cosmogenic nuclide is produced in situ in a solid, e.g., ^{10}Be in rock; (2) closed systems in which the in situ production has stopped because of the complete shielding of a sample from cosmic rays, e.g., $^{26}Al/^{10}Be$ in deeply buried quartz; and (3) a now-closed system that formerly was in equilibrium with a reservoir that had a constant or known concentration of a cosmogenic nuclide, e.g., ^{14}C in *any* biogenic material; the reservoir is either the atmosphere or ocean.

This entry treats the open system and closed system (1 and 2) applications of nuclides specifically produced in exposed minerals near Earth's surface, to determine an exposure age of a surface, burial duration of minerals, or erosion rate of surfaces and catchments (Lal, 1991). The term *terrestrial in situ cosmogenic nuclide* (*TCN*) exposure history describes this method, which utilizes a growing knowledge of how production rates spatially and temporally vary on Earth owing to variations in the geomagnetic field and atmospheric shielding. TCN methods are distinguished from methods using meteoric cosmogenic nuclides, even when the latter are absorbed by clays in soil and marine sediments or accumulated in various water reservoirs (e.g., ice sheets, groundwater). The term *CRN* excludes the stable cosmogenic nuclides (e.g., ^{3}He, ^{21}Ne, ^{38}Ar), *SED* can be achieved with other dating methods (e.g., luminescence), and *CRE* dating can be conducted on lunar and other planetary surfaces.

The TCN dating method is a *numerical dating method*. Currently the TCN production rates have been calibrated against other dating methods owing to the difficulty of obtaining precise cross sections for the production of each isotope through different interaction pathways. This would suggest that it is calibrated, such as

lichenometry or the geomagnetic secular variation dating method. However, with improvements in our understanding of the temporal and spatial variations in the geomagnetic field, cosmic ray interactions, nuclear cross sections, production rates, and depth profile shapes are becoming reliably predicted by theory (Masarik and Reedy, 1995; Argento et al., 2013). In this sense, the TCN dating method is a numerical, *not calibrated*, method. The TCN method is distinct from cosmogenic dating methods based on correlation. For instance, meteoric cosmogenic nuclides measured in time series media – such as ^{10}Be in glacier ice (Beer et al., 1987) or marine sediment (Morris et al., 2002) – can provide a reliable method for correlating undated records to meteoric cosmogenic nuclide records in independently dated cores.

Introduction

TCN exposure methods are used to determine the duration of exposure to cosmic rays, duration and degree of shielding from cosmic rays, and rate and style of erosion, on or near Earth's surface. The premise is that the measured concentration of TCN is proportional to the duration that the mineral has been exposed to cosmic rays (Figure 1) and, in the case of a radioactive TCN in a shielded sample, how much time the concentration has decayed.

Depending on the energy and type of incident cosmic ray particle and target nucleus, cosmic ray interactions produce a variety of secondary particles over a wide energy spectrum, including gammas, electrons, kaons, pions, muons, neutrons, protons, deuterons, tritons, ^{3}He nuclei, alphas, and heavier nuclides. It is the heavier nuclides that are of interest. However, to be useful for exposure dating, the TCN should:

- be stable or have suitably slow decay rates
- be more abundant than the radiogenic or nucleogenic species in the target mineral
- have in situ production rates that yield extractable concentrations that can be resolved against its elemental isotopes
- be precisely measurable considering blanks, detection limits, and isobaric interferences
- be produced in stable, chemically resistant minerals that are common and have low thermal diffusivities for noble gases at surface temperatures.

This greatly reduces the number of useful particles, and currently only 6 TCNs are widely used: ^{3}He, ^{10}Be, ^{14}C, ^{21}Ne, ^{26}Al, and ^{36}Cl (Table 1). The probability for cosmic ray interaction – cross section, measured in barns – takes into account the type and energy of the incident secondary and target nuclei. Thus, each TCN is produced at a unique rate, depending on the energy of the cosmic radiation, the type of interactions of which there are five (spallation, thermal and epithermal neutrons, and interactions of negative and fast muons), and the chemistry of the mineral. Although quartz is the most commonly used mineral, other minerals include calcite, feldspar, garnet, hornblende, magnetite, olivine, pyroxene, and sylvite. With the general exception of quartz, the chemical composition of each mineral should be measured to determine the abundance of suitable target nuclei for each of the five interactions. Quartz is unique in that its composition is stoichiometric, eliminating the need to analyze its chemical composition to determine the different production rates. For instance, ^{10}Be is produced in quartz from spallation and muonic interaction on Si and O at a rate of about 4 atoms g^{-1} year^{-1} at sea level, high latitude, under current atmospheric and magnetic field conditions. Until recently, even whole rock samples have been analyzed for ^{36}Cl, ^{10}Be, and ^{14}C, giving the possibility that any lithology can be used if the TCN production rates for the specific rock composition can be determined. Thus, every TCN-mineral system is a unique clock. Ratios of multiple TCN can be measured in a single mineral (e.g., ^{10}Be, ^{14}C, ^{21}Ne, and ^{26}Al in quartz, Figure 1) or in the same rock (^{36}Cl in feldspar and ^{3}He in olivine in basalt).

The TCN exposure methods differ from other dating methods. Both radioactive and stable (noble gas) isotopes can be used. The concentration of the isotopes is generally depth dependent, unlike other radiometric chronometers which are dependent on the parent isotope abundance. The technique is not temperature dependent as is the case for thermochronometry and amino racemization. Unlike most geochronometers, the TCN method is not necessarily restricted to specific minerals with a certain isotopic abundance, although production rates are currently well known for relative few minerals.

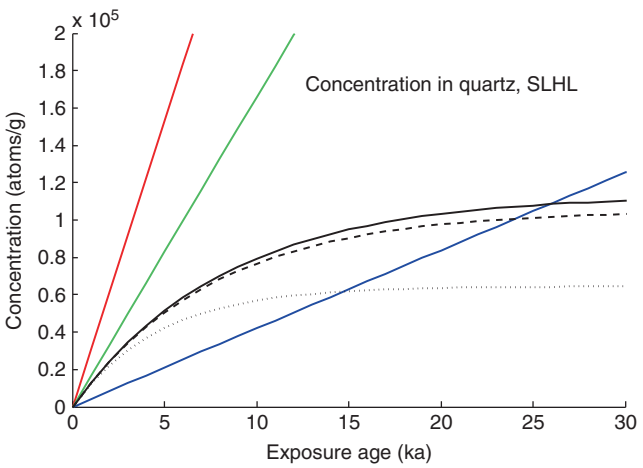

Terrestrial Cosmogenic Nuclide Dating, Figure 1 Gradual buildup of four TCNs in quartz at sea level high latitude. *Black*, ^{14}C; *green*, ^{21}Ne; *blue*, ^{10}Be; and *red*, ^{26}Al. Continuous production by spallation only, with rates according to Borchers et al. (submitted) and Kober et al. (2011). *Solid lines* represent surfaces with zero erosion. Constant continuous erosion of 5 and 10 mm ka^{-1} shown with dashed and *dotted curve* for ^{14}C.

Terrestrial Cosmogenic Nuclide Dating, Table 1 Commonly used terrestrial cosmogenic nuclides

Nuclide	ET	ATM	Half-life (ka)	Isotope	Isobar	TCN analysis	TCN production mechanisms	Target minerals
^{3}He	•		Stable	^{4}He	^{3}H	NGMS	nf	Ol
^{10}Be	•	•	1,390	^{9}Be	^{10}B	AMS	nf, μ	Qtz
^{14}C		•	5.73	$^{12/13}$C	^{14}C	AMS	nf, μ, nt	Qtz
^{21}Ne	•		Stable	$^{20/22}$Ne		NGMS	nf, μ	Qtz
^{26}Al	•	•	720	^{27}Al	^{26}Mg	AMS	nf, μ	Qtz
^{36}Cl	•	•	300	$^{35/37}$Cl	^{36}S	AMS	nf, nt, μ	K, Ca-rich

Notes
Cosmogenic $^{37-38}$Ar is not listed as it is not widely used as a TCN owing to difficulties in isolating it from the radiogenic components
ET, ATM: these nuclides are also measured in extraterrestrial and atmospheric/meteoric targets
Isobar: listed are the most important isobaric interferences; recent isobaric separation innovations have greatly reduced the impact of isobars on low-level TCN measurements
Production pathways: nf, spallation by fast neutrons; nt, thermal (and epithermal) neutron capture; μ, fast and negative muonic interactions
Target minerals: only the most commonly utilized minerals are listed. For ^{36}Cl and $^{37-38}$Ar feldspar separates are now used more than whole rock

Examples of TCN exposure and burial dating

Details of the measurement and interpretation of TCN are provided below. Table 2 provides an indication of the wide range of applications of the method. Currently the most widely used application of TCN methods is exposure dating of glacial boulders for moraine chronologies, followed by the application of TCN to provide age control on alluvial strain markers for fault kinematics, and catchment average erosion rates.

Range of applicability

The applicable range for TCN dating crosses seven orders of magnitude – more than any other dating method. Theoretically, the lower limit of the surface exposure dating method is ~10^0 years. While exposure ages of years have been determined, the technique is practically limited by the difficulty of measuring low concentrations (i.e., few hundreds of atoms per gram of mineral, requiring a large sample mass) and our knowledge of production rate controlling factors such as atmospheric dynamics and the geomagnetic field variations over such a short integration time. Although the stable noble gas cosmogenic isotopes do not decay and have low thermal diffusivities in selected minerals at the Earth's surface, an effective upper dating limit on Earth is 10^7 years (e.g., alluvial surfaces in the Atacama Desert, Dunai et al., 2005). This is because the concentration of cosmogenic nuclides typically decreases with depth and because all surfaces on Earth over such long exposure durations will experience erosion. The applicable range for burial dating with ratios of TCN is narrower because short periods of shielding cannot be distinguished from the effects of erosion on the ratio.

The range of erosion rates over which the technique is applicable is narrow and depends on the approach, isotope-mineral system, and measurement precision. Surface erosion rates of continually exposed bedrock approaching 0.01 mm ka^{-1} can be determined with analytical precisions (~3 %) and are usually averaged over a wide exposure time. Faster erosion rates, up to a maximum of 10^3 mm ka^{-1} for rock, may be resolved in the rare instance that the erosion rate is constant over much shorter exposure durations. Only recently has the TCN method been able to establish rates of the complex situation of nonconstant episodic erosion.

The TCN dating method extends beyond the normal limits of common Quaternary dating methods such as radiocarbon (5×10^4 years) and luminescence (10^5 years). Therefore, the technique provides a useful bridge between Quaternary and older dating methods. Furthermore, its ability to determine erosion and burial histories over the past 10^7 years can support exhumation models based on thermochronology.

Historical developments

While the TCN dating method became established in the mid-1980s, the theory of the geochronometer was developed much earlier. Following the discovery of X-rays and radioactivity at the turn of the nineteenth century, experiments were undertaken to establish how high above Earth's surface atmospheric ionization would continue. As observation heights increased from towers to balloon experiments more than 5,000 m high in the atmosphere, it became apparent that above a few hundred meters the ionization rate actually increased with height and that the radiation did not diminish at night or during an eclipse. The demonstration of a non-terrestrial and nonsolar radiation (ionization with constant day and night and during an eclipse, Hess, 1912) initiated a new field of physics. Two decades later, the first cosmic "radioelement" measured in rock was protactinium in eucolite and eudialyte, collected from surface outcrops in Greenland. Grosse (1934) carefully demonstrated that the amount of protactinium from the already well-established U-series decay rates was more than 3 % higher than the parent activity could explain. He indicated that a better understanding of the interaction of cosmic rays with matter and cosmic

Terrestrial Cosmogenic Nuclide Dating, Table 2 Examples of applications of TCN methods

Method	Landform/material	Purpose/test
Exposure dating	Lava surface	Eruption age or recurrence rate
	Bedrock fault scarp	Variation in slip rate with time
	Landslide scarp face	Acceleration of mass movement
	Erratics on moraine, esker, or plain	Timing of deglaciation, retreat rate
	Boulders on alluvial fan	Age of strain markers for fault kinematics
	Boulders on a beach	Isostatic uplift rate or tilt rate of raised shorelines
	Impact ejecta	Age of impact
	Bedrock mountain peaks, tors	Age of formation, timing of last glaciation
	Precariously perched boulders	Timing of seismicity for a given acceleration
	Overturned boulders	Timing of last major flood event
	Colluvial blocks	Timing of last seismic shaking
	Submarine cobble on continental shelf	Duration of shelf exposure
	Debitage, quarried tools	Timing of human occupation
Depth profile dating	Multiple sand samples in a terrace	Stream incision rate, age of strain marker
	Multiple samples in raised delta foresets	Relative sea-level curve, timing of marine limit
Burial dating/isochron dating	Sediment in caves	Burial age of associated fossils, stream piracy
	Lava stack	Eruption recurrence rate
	Sediment buried under sediment	Age of paleoecological, paleontological, or anthropology records
	Cobbles buried by water	Duration of transgression
	Bedrock or sediment in glaciated area	Duration of cold-based ice cover
Erosion rate	Single rock surface	Outcrop-scale maximum constant erosion rate
	Single outcrop with TCN at saturation	Outcrop-scale average constant erosion rate
	Modern stream sediment	Average erosion rate for catchment above sample
	Older fluvial sediment	Paleo-erosion rates of catchment above sample
	Sediment sample	Erosion rate of surface with short-lived TCN
	Multiple samples in a depth profile	Erosion rate of sediment surface
	Two adjacent samples at different depth	Episodic erosion rate on glaciated summits
Paleoaltimetry	Single lava surface of known age with large vertical offset	Rate of offset
	Rapidly uplifted surface	Rate of uplift using atmospheric depth-dependent ratio of TCNs

radiation variation with time was necessary to fully understand the production of cosmic radioelements. Knowledge of cosmic ray flux and interactions continued only through measurements of cosmogenic nuclides at higher concentrations in meteorites, lunar samples, and meteoric samples (tree rings, manganese nodules, ice sheets) and sophisticated transport codes capable of simulating particle interactions at various energies and magnetic field (Reedy et al., 1983). A current and very comprehensive review by Olive et al. (2014) provides the state of knowledge of the particle physics and cosmology underlying the theory.

Measurement of TCN lagged the theory. The low production rate of cosmogenic nuclides on Earth's surface even at mountain elevation (hundreds of atoms per gram of mineral per year) resulted in few successful measurements of TCN (Davis and Schaeffer, 1955; Hampel et al., 1975) until significant improvement in isotope mass spectrometry. Unlike radiocarbon dating (based on the decay of ^{14}C produced in atmosphere by cosmic rays and invented by Willard Libby in 1948), application of TCN methods has only been practical since the advent of improved spectrometry of noble gas isotopes and ultimately accelerator mass spectrometry (AMS) in 1977. The technical difficulty lies in the accurate measurement of an extremely small number of atoms, typically 10^6 to 10^8 in a sample that might range from a few milligrams ($\sim 10^{19}$ atoms) to a kilogram of material ($\sim 10^{25}$ atoms). Even after extracting and concentrating the chemical moiety of interest, say aluminum for ^{26}Al measurements, the isotopic ratios are still daunting, $<10^{-14}$.

During an experiment in which atmospheric ^{10}Be (half-life 1.39 Ma) was used as a radioactive tracer to prove that pelagic sediments from the ocean floor were carried through the subduction zone, and ultimately incorporated in the lavas erupted by arc volcanoes, Brown et al. (1982) obtained high concentrations (1×10^6 atoms g^{-1}) of ^{10}Be in the Columbia Plateau basalt. The Columbia Plateau basalt had been chosen as a control sample: since it was produced by hot-spot volcanism which has no connection with subduction, sediments, or any other "surface" material, it was expected to be a blank ($<10^2$ atoms g^{-1}). All other samples from hot-spot volcanism in Hawaii and Iceland had been blank. The significant difference between the Columbia Plateau sample and these other samples was that the other samples were collected within a year

of their eruption, sometimes days, while the Columbia Plateau sample had lain subaerially exposed for 14 Ma. It was first thought that the ^{10}Be contamination might be meteoric ^{10}Be, brought to the basalt by rain. But sequential etching of the surface proved that the "contamination" was distributed uniformly throughout the sample. The only remaining possibility was that the ^{10}Be was produced in situ as the sample lay on the surface. A quick calculation showed it was possible. This was the first measurement of an in situ-produced terrestrial cosmogenic nuclide with modern methods. Shortly after, five papers in 1986 announced the birth of TCN exposure history and erosion methods (Craig and Poreda, 1986; Klein et al., 1986; Kurz, 1986; Nishiizumi et al., 1986; Phillips et al., 1986). The number of different applications of the TCN method has continued to grow (Table 2; for reviews, see Lal, 1991; Gosse and Phillips, 2001; Dunai, 2010; Granger et al., 2013).

Since Lal's seminal 1991 paper, the number of parameters considered when interpreting the TCN data has increased, and uncertainty in their values has improved. During the last three decades, the community has benefitted from over a hundred studies from both individual and group efforts to improve sampling strategies, isotope geochemistry procedures, our knowledge of production rate through the atmosphere and lithosphere, and our capacity to process the data. The community shared a number of different calculators – e.g., CHLOE for ^{36}Cl ages, erosion rates, and depth profiles (Phillips and Plummer, 1996), CosmoCALC for ages with any of the TCN (Vermeesch, 2007), and a Bayesian-like Monte Carlo-based calculator for depth profile dating (Hidy et al., 2010). The most significant development began in the mid-2000s, when two multinational programs were funded for the primary purpose of improving our knowledge of TCN systematics. CRONUS-Earth was funded by the US National Science Foundation and CRONUS-EU was funded by the European Union. Early in the process, an online calculator was provided by members of the CRONUS-Earth group (Balco et al., 2008). Over the last decade, important data gaps were filled and improvements in our understanding were made in nuclear cross sections, radioactive decay rates, muonic interactions, spatial scaling of production rates, temporal variations in production rates, and a more robust assessment of error. The results of these programs have been recently published or submitted (Phillips et al., 2014 submitted). One major improvement is the manner in which the secondary flux is scaled through the atmosphere and the changing geomagnetic field (Lifton et al., 2014). An updated CRONUS online calculator is available at http://web1.ittc.ku.edu:8888/. Currently there remains a lack of consensus regarding some aspects of the computation used in this and other calculators and the values of some of the parameters chosen, particularly the production rates. Although the CRONUS programs have ended, efforts to improve the TCN methods continue.

TCN dating systematics

TCN production pathways

At the base of the atmosphere, the most abundant secondaries capable of producing TCN are neutrons and muons. Other secondaries either lack energy, have rapid decay rates, are uncommon, or are absorbed so quickly in the atmosphere that they generate TCN at a much lower rate. TCN are produced in exposed minerals by three main interactions: spallation by high-energy neutrons, capture of thermal or epithermal neutrons, and muonic interactions.

At the base of the atmosphere, at sea level, the most abundant cosmic ray is muons with an average energy of 4.2 GeV. They have a vertical flux of ~70 m^{-2} s^{-1} sr^{-1} (for momentum > 1 GeV c^{-1}); incident on a horizontal surface, the equivalent flux is ~1 cm^{-2} min^{-1}. Nucleons are the next most abundant: the integral vertical intensity of protons above 1 GeV c^{-1} is ~0.9 m^{-2} s^{-1} sr^{-1} and for neutrons ~0.45 m^{-2} s^{-1} sr^{-1}. Other components of the flux including the electromagnetic pions and kaons play a little role in the production of TCNs.

Spallation

A spallation reaction occurs when a low-mass (e.g., neutron, proton) energetic (>30 MeV) particle interacts with a nucleus. The interaction causes an intranuclear or hadronic cascade that at first evaporates neutrons and protons and other light nuclei and then may eventually result in the breaking apart (fission) of the target nucleus. In general, the most probable products have masses close to the target nucleus or close to the projectile. All TCNs are produced by spallation, and it is the dominant production pathway for TCN within the upper 1,000 g cm^{-2} (~4 m) of the lithosphere.

Thermal and epithermal neutron capture

Neutron capture occurs when a slow neutron is absorbed by a nucleus to create a nucleus with a mass of one amu larger. Fast neutrons lose their energy through momentum transfer during elastic collisions with nuclei. Epithermal neutrons (0.1 MeV to 0.5 eV) and thermal neutrons (<0.025 eV) can be captured by a nucleus. The resulting nucleus is generally unstable and it decays by the immediate emission of a proton, or beta decay. Excited nuclei relax by emission of a gamma. While thermal-neutron capture is possible by many nuclides, the only cosmogenic nuclides that are produced significantly by thermal-neutron capture are ^{14}N(n, p)^{14}C, ^{35}Cl(n, γ)^{36}Cl, and ^{40}Ca(n, γ)^{41}Ca.

Muonic interactions

Muons (leptons that are 207× more massive than electrons) are produced in cosmic ray showers from the decay of mesons and comprise more than eighty percent of the non-electromagnetic cosmic ray flux at Earth's surface. However, like other leptons, they do not interact through the strong force and thus their penetration is much greater

than neutrons. Despite their short half-life (10^{-6} s) and their relatively small contribution (<2 %) to total TCN production at the lithosphere surface, slow negative muons (*e*-folding length Λ ~1,300 g cm^{-2}, Heisinger et al., 2002a) and fast muon (Λ ~4,320 g cm^{-2}, Heisinger et al., 2002b) are the dominant production pathways at depths greater than 4 m in rock (>1,000 g cm^{-2}). For comparison, the Λ for fast neutrons is ~145 g cm^{-2}. Muon contributions to TCN production are therefore important when applying TCN burial dating methods or when samples are collected from rock or sediment depths greater than 1 m.

TCN production

Exposure duration (t) of a basalt boulder on a moraine is determined by the measurement of the TCN concentration in a target mineral, such as ^{3}He in pyroxene:

$$t = \frac{C_{meas} - C_i}{P_{T,t,0}} \quad (1)$$

where C_{meas} is the measured abundance of ^{3}He per gram of pyroxene, C_i is any concentration of ^{3}He that is either non-cosmogenic or in situ cosmogenic ^{3}He produced prior to the deposition of the boulder on the moraine (i.e., "inherited concentration"), and $P_{T,t,0}$, the total production rate at the surface, is the time-integrated sum of all cosmogenic nuclide production pathways for ^{3}He in pyroxene at the surface for the particular time, in atoms g^{-1}a^{-1}.

The state of knowledge of production rates and how they scale spatially and temporally is rapidly improving (Lifton et al., 2014; Phillips et al., 2014 submitted). Site-specific time-integrated production rates have been determined (calibrated) by measuring TCN concentrations in minerals with simple exposure histories over an independently determined duration (C_i is considered zero or is measured). The sum of production rates from the different cosmogenic nuclide interactions (fast neutrons, P_{nf}; thermal neutrons, P_{nt}; epithermal neutrons, P_{ne}; negative muons, $P_{\mu n}$; and fast muons, $P_{\mu f}$) depends on the nuclide-target system, location, environmental factors, and the particular part of Earth's geomagnetic field and atmosphere history corresponding to the exposure period. For reference, the calibrated TCN production rates are scaled to sea level, high latitude, under today's geomagnetic and atmospheric conditions (e.g., ^{10}Be is produced in quartz at ~4 atoms g^{-1} year^{-1}). Thus, first-order (up to two orders of magnitude) adjustments to the reference production rate may be required to account for spatial variability in atmospheric and geomagnetic controls on the cosmic ray flux to any location on Earth.

Earlier simplifications with a symmetric standard atmosphere and dipolar magnetic field have now been replaced by more sophisticated models for both. In general, lower magnetic field strength will result in a higher production rate and a softer (lower average) secondary energy spectrum that will not penetrate as far. Sites at higher geomagnetic latitudes have higher surface production rates. The flux of each type of secondary decreases with penetration through the atmosphere, so production rates decrease with atmospheric depth. Atmospheric shielding is a greater control than geomagnetic field effects (except during reversals) so the highest production rates are at mountain tops.

The intensity and geometry of the geomagnetic field and the distribution of atmospheric mass has changed with time. The effects can cause changes of >25 % over several millennia for a given site. Periods with higher paleointensities had lower instantaneous TCN production rates. During colder periods when the atmosphere contracted, production rates at high altitudes were less shielded. Such temporal variation in production is clearly evident from the variation in abundances of atmospheric ^{14}C or ^{10}Be abundances recorded in ice sheets or marine sediments. Fortunately, unlike the instantaneous effect of these changes on atmospheric cosmogenic nuclide production used for radiocarbon dating, terrestrial in situ production is integrated over the entire exposure duration, so TCN dating is not as sensitive to short-term high-amplitude geomagnetic or atmospheric variations.

Other first-order adjustments are needed to account for the decrease in production as the average energy of each type of secondary flux decreases with mass depth z (g cm^{-2}) through rock:

$$P_{z,nf} = P_{0,nf} e^{-z/\Lambda_{nf}} \quad (2)$$

where P_0 is the surface production rate and Λ_{nf} is the effective *e*-folding attenuation length for fast neutrons at that depth. While the concentration of TCN produced from spallation by fast neutrons generally follows this simple exponential, thermal-neutron capture interactions do not. Owing to the moderating effect of water (water vapor in air, pore water in rock or sediment, snow cover) on thermal neutrons, initially there is a reduced thermal and epithermal neutron flux in the upper 60 g cm^{-2} of rock or sediment until the flux re-equilibrates with the exponentially attenuating fast neutron flux. Unlike spallogenic TCN, the highest concentration of thermal-neutron capture TCN occurs a few dm below the surface.

Second-order adjustments to the production rate may be negligible or significant. These include corrections for erosion or exhumation of the samples, cover by snow, water, ice, loess, or colluvium (shielding the surface from fast neutrons); geometry of the sampled surface; partial shielding by vegetation; elevation changes due to isostatic, tectonic, or surface processes; and partial shielding of cosmic ray secondaries due to topography.

Laboratory and field considerations

The field and laboratory procedures will depend on the objective of the study. Choices of TCN will mainly depend on the abundance of target minerals with known production rates, the radionuclide half-life, and whether

or not multiple nuclides or a particular production pathway is sought.

There is no standardized list of field observations for TCN methods, partly because the types of TCN applications vary widely. Table 3 includes most of the important observations that will be needed to calculate an age or erosion rate, adjust for complexities in exposure history, interpret the data, and evaluate uncertainty. The number of samples necessary will depend on many factors. If inheritance is possible (e.g., due to exposure prior to the

Terrestrial Cosmogenic Nuclide Dating, Table 3 Field observations

Observation	Example	Comment
Latitude	−72.4472°	Convention: south is negative; high precision is useful for site recovery
Longitude	−130.3362°	Convention: west is negative; high precision is useful for site recovery
Elevation	3,232 m	Record method; evidence for surface elevation changes during exposure should be considered
Pressure	Varies	Used if atmospheric model does not adequately describe the time-averaged barometric pressure for the average temperature history
Bulk density	2.7 g cm^{-3}	Bulk density of the material sampled; if subsurface sampling, bulk density of the material above each sample must also be determined
Thickness	1.0 cm	Average thickness of the sample
Depth below top	0 cm or 10 g cm^{-2}	For surface samples, this is taken as 0 cm. For subsurface samples, the vertical distance between the landform surface and the top of the sample is recorded. Units vary with calculator
Surface slope	19° → 235°	This is the dip and dip direction of the slope of the sampled surface. Generally dips less than 10° will have negligible foreshortening effects, unless there is considerable topographic shielding
Topographic shielding	235, 310, 40, 130, 170° 22, 13, 9, 17, 25°	Trend and plunge (°) measurements taken at major topographic inflections in the skyline. This shielding becomes more critical with greater shielding (e.g., in a canyon) and with greater sampled surface slope
Sample height	130 cm; geometry	If the surface of the sampled landform is above the local ground level, such as a boulder top, it may be useful to provide the entire geometry (L, W, H) when considering neutron loss
Snow shielding	100 cm for 3 months, 50 cm for 2 months, 0.25 g cm^3	An estimate of the thickness and density of snow that may have covered the sampled surface. If the surface is above the local ground level, consideration for the sample height may be required
Geometry effects	30 cm from edge; 25 cm under an overhang that protrudes 80 cm from cliff	This is needed to compute effective attenuation lengths, compute thermal-neutron production rates, and evaluate neutron loss
Forest shielding	Temperate rainforest for majority of time	Record the type of forest and other vegetation cover. For boulders, this could account for 2 % to >9 % shielding of secondary cosmic ray flux (e.g., boreal forest or temperate rainforest). For subsurface samples, vegetation shielding could be even greater
Erosion	1 mm ka^{-1}; 30 cm max	If known, indicate method or evidence (height of protruding quartz vein; striation; soil development; lichen cover; weathering features; measured). Units vary with calculator
Aggradation	50 cm	Gradual or episodic cover by loess, ash, colluvium, ice, water, and other material currently or previously existing that was added to the surface of the landform after exposure began
Sample type	Boulder; braided stream deposits	Describe lithology, sediment structures
Landform type	Broad moraine ridge; fluvial terrace	Provide stratigraphy information, e.g., Qf3. Describe where on the landform the sample was collected (subsurface samples under a longitudinal bar in the alluvial fan)
Sample method	Cutoff saw; chisel; hand dug pit	Indicate any difficulties, particularly if thickness is not constant
Inheritance	High catchment erosion	Note evidence of catchment erosion for sediments (e.g., alluvial fans); low rates may indicate a higher probability of inheritance, yielding older apparent ages or causing scatter among individual ages on a given landform
Volumetric water	5 % water content in soil	The volumetric water content, Qv, is needed to account for moderation of the thermal and epithermal neutron flux through rock and sediment. Each sedimentary layer and soil horizon may need its own measurement
Soil properties	15 cm below the 30 m mixed zone	Information about the soil that can help constrain erosion rate (e.g., a local catena, or evidence that the soil has been truncated); evidence that the samples were collected below any zone of cryoturbation or bioturbation; consideration that a soil horizon may have gradually altered the bulk density and moisture properties over time
Exhumation of the surface	Cobble may have been frost heaved, or till may have been eroded	Boulders and small clasts may have moved vertically in the sediment and been completely exposed for a shorter time than the actual landform. Exhumation by frost heave or denudation of the landscape should be noted

exposure period of interest), concordance of three or more surface exposure ages may be required to establish if inheritance is negligible, or subsurface samples in sediment collected in a depth profile may be needed to adjust for the average inheritance of a sediment.

While the physical and chemical processing required will vary with the isotope-mineral system, the objective is the same: provide a pure and representative target with sufficient TCN concentration to obtain the desired precision. Mineral isolation processes after cleaning, crushing, grinding, and sieving include froth flotation; magnetic, electrostatic, heavy liquid, air abrasion; and differential leaching with hydrofluoric, hexafluorosilicic, or hot phosphoric acid. For the noble gas measurement, no future chemistry may be required on the <100 mg of target mineral. For AMS, extracting and concentrating the radionuclides after dissolution is achieved with isotope dilution (spiking) followed by dissolution, ion chromatography, and pH-controlled precipitation, yielding BeO, Al_2O_3, AgCl, or other targets which are mixed with a pure metal to enhance sputtering in the AMS source. Masses between 2 and 200 g will be needed, depending on the concentration. Extraction of ^{14}C is by thermal extraction of ^{14}C in the presence of ultrapure O and can be in graphite or CO_2 gas. Most extraction methods require less than 10 g of quartz. Some elemental analyses of the naturally abundant isotope or a measurement of target nuclei abundances, radiogenic and nucleogenic sources, or neutron moderators is usually required.

TCN applications: dating of surfaces and sediments with simple exposure histories

Exposure dating has been conducted in just about every landscape element to address questions relevant to classical geomorphology, landscape responses to climatogenic and tectonic change, kinematics of brittle and ductile deformation, and applied science regarding geohazard risks associated with seismicity, volcanism, mass wasting, aridity, and sea-level change. Various combinations of isotopes and sampling strategies can reduce the degrees for freedom in constraining the factors that control the calculation of an exposure or burial age.

Single-nuclide surface exposure dating

A simple exposure age on a surface that is not eroding can be determined with a stable or radionuclide with decay constant λ:

$$t = -\frac{1}{\lambda}\ln\left(1 - \frac{C\lambda}{P}\right) \tag{3}$$

However, if the surface experienced a constant erosion or aggradation during the equation, it is more complicated. Constant erosion and aggradation can be treated explicitly. As the absorption of the cosmic ray secondaries with mass is well known, we are not required to sample at the surface. An approximation for the concentration of a nuclide in a rock at depth z (cm) with an erosion rate ε (cm a^{-1}) was provided by Lal (1991)

$$C_{(z,t)} = \frac{P_{(t,0)}}{\lambda + \frac{\rho\varepsilon}{\Lambda}}\, e^{\frac{-\rho z}{\Lambda}}\left(1 - e^{-\left(\lambda + \frac{\rho\varepsilon}{\Lambda}\right)t}\right) + C_{(z,inh)}e^{-\lambda t} \tag{4}$$

The latest CRONUS calculator (Borchers et al., submitted) iteratively seeks an exposure time with a set of equations that allow production rates through the five interaction pathways to vary over the exposure period, simultaneously considering changes in effective attenuation lengths during erosion. If erosion rate is known and constant, exposure age can be solved. However, if the erosion rate is uncertain or appears to be episodic, the normal protocol with a dominantly spallogenic TCN is to assume $\varepsilon = 0$ to obtain a minimum exposure age for the surface. If the inherited concentration ($C_{(z,inh)}$) is also not negligible, but erosion is zero, the exposure age would be a maximum age. The exposure age cannot be constrained with one isotope (maximum nor minimum limit) if both inheritance and erosion are nonzero. However, if single-nuclide exposure ages from multiple, spatially distinct samples from the same landform are identical, then it may be possible to suggest a negligible inheritance in all samples.

Multiple nuclide surface exposure dating

To overcome the difficulty related to erosion, two nuclides can be measured in the same rock surface. If the surface has been exposed and eroding at a steady state for a long time, the concentration of radionuclides will reach a dynamic equilibrium where loss due to decay is matched by the production according to the above equation. A short-lived radionuclide that has reached its saturation concentration C^* for a given erosion rate over sufficient time can be used to determine the erosion rate (Lal, 1991):

$$\varepsilon = \frac{\Lambda}{\rho}\left(\frac{P}{C^*} - \lambda\right) \tag{5}$$

The surface exposure time can be determined by adjusting the unsaturated concentration of a second nuclide for this erosion rate. Alternatives to the saturation approach include a combination of a TCN with a significant thermal-neutron capture production rate (e.g., ^{36}Cl) and a spallogenic isotope (e.g., ^{10}Be). The thermal-neutron loss near the surface will cause the concentration to increase with erosion, while the spallogenic nuclide will decrease for the same erosion rate. Their erosion-adjusted ages will converge provided that erosion rate is not too fast and that sufficient ^{35}Cl is in the mineral.

The two-isotope approach can also solve exposure age and erosion rate simultaneously for two radionuclides without the need for saturation or thermal-neutron production (Figure 2). However, the $^{26}Al/^{10}Be$ ratio plot (Nishiizumi et al., 1986) reveals a narrow banana-shaped

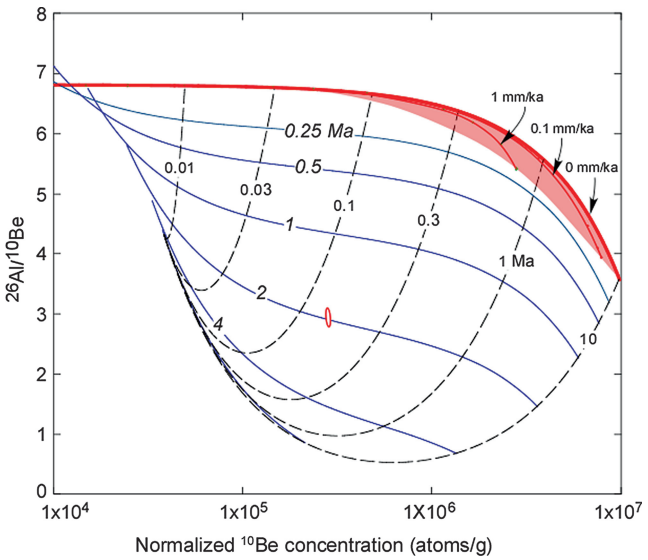

Terrestrial Cosmogenic Nuclide Dating, Figure 2 $^{26}Al/^{10}Be$ versus ^{10}Be plot. Production systematics as per Balco et al. (2008) for the Lal (1991) and Stone (2000) time invariant scaling model, initial ^{10}Be production rate of 4.9 atoms g^{-1} and surface $^{26}Al/^{10}Be$ of 6.75, and muogenic production from negative and fast muons (Heisinger et al., 2002a; Heisinger et al., 2002b). Plot and sample represent a surface of 30 m depth under gravel with 1.9 g cm^{-3} density. The thick red upper curve represents the history of a sample that experienced continuous exposure with no erosion (exposure duration in Ma increases to the right). Ratios plotting within the shaded field ("steady-state erosion field" (Lal, 1991)) have experienced erosion or minor burial (curves indicated for 0.1 and 1.0 mm ka^{-1} constant and continuous erosion). Samples plotting below the shaded field have experienced a complicated exposure history in which an exposure was by at least interrupted one burial event. Even at 30 m, the shielding is not complete because of muogenic production. The duration of burial indicated by the thin blue curves ranging from 0.25 to 8 Ma represents the burial age for a single even or a minimum estimate of burial duration if multiple burial events have occurred, as in cyclic glacial cover. The hypothetical sample shown with 1σ error ellipse could be interpreted to represent a minimum exposure duration of 0.2 Ma and minimum burial duration of 2 Ma. However, it is possible that the sediment was buried and reexposed many times, so the total time represented would be greater than 2.2 Ma. If an amalgamated sediment had a depressed initial ratio (owing to complex exposure prior to final deposition), then the burial age would overestimate the timing of the last burial event.

steady-state island and therefore requires very high precision to establish erosion and exposure age. Phillips et al. (1997) have suggested that the $^{10}Be/^{36}Cl$ may have the advantage of being more sensitive for experiments requiring simultaneous solutions of exposure age and erosion rate. Ratios of a noble gas and radionuclide have also been used, and a three-isotope approach may have the advantage of a reduction of a degree of freedom. The multi-isotope approach may also simplify the requirement to know how production rates have changed with time if, in some circumstances, the amount of variation is the same for all measured isotopes in the same sample.

Exposure dating of sediments

The difference between dating the exposure age of a rock surface and dating the depositional age of a sediment is that each grain of the allochthonous sediment will have a different C_{inh} which must be considered in the calculations. There are many approaches to dating a sediment (see Gosse, 2012 for a review). If the objective is to determine the age of a cut or fill alluvial terrace surface, a fan or delta surface, moraine, or mass wasting deposit, it is possible to date large boulders (reducing the effect of snow or loess cover and exhumation) or cobbles and pebbles on the surface. As in dating a bedrock surface, a single-nuclide age on a clast (or amalgamation of clasts) on the surface of a deposit requires knowledge of erosion (or aggradation) history and inheritance.

Erosion of the surface can be determined by different TCN approaches as discussed above. An alternative approach is to use subsurface samples. The concentration versus depth profile through a rock or sediment is controlled by erosion rate. The faster the erosion rate, the steeper the profile until ultimately only a fast muonic attenuation would be measured. Unfortunately, constant erosion rates on Earth are generally not that fast, so most measured depth profiles will be dominantly controlled by the simple *e*-folding length for a fast neutron. Therefore, a single spallogenic nuclide cannot establish a unique erosion rate or exposure age. However, a depth profile for a single TCN with sufficient thermal-neutron capture production (e.g., ^{36}Cl) can provide this uniqueness. Alternatively, two TCNs can be measured in the same profile to solve for erosion rate and age (Mercader et al., 2012).

The C_{inh} in sediment clasts is equally problematic. If not treated, the apparent exposure age will overestimate the actual timing of deposition. There are many approaches, each with assumptions that may be validated in certain scenarios. One option is to measure the exposure age for many samples on the surface of the deposit and assume that all clasts have been eroded similarly. If there is no variability among ages, then it may be possible to interpret that inheritance is negligible, as it is very unlikely that all clasts would have the same inheritance if the C_{inh} was a significant component of the total concentration. This is often the case where sediment is eroded from glaciated catchments or regions with otherwise very high erosion rates. In regions where the sediment is sourced from a catchment that has not been rapidly eroded, determining the C_{inh} is necessary. One option is to measure a sample that is essentially shielded from cosmic rays (e.g., >4,000 g cm^{-2} deep) for long exposure to muons (Brown et al., 2002) and assume that the sediment at shallower depths have the same C_{inh}. This assumption would only be true in special cases where, for instance, the sediment flux from the catchment remained constant

over that entire thickness. A similar approach that uses the TCN concentration in modern stream sediment as an indication of C_{inh} is similarly invalid for many catchments in which millennial-scale climate variations have changed catchment erosion rates. A better and more widely used treatment of inheritance in alluvium (Anderson et al., 1996) uses the TCN concentration in at least four subsurface samples of amalgamated clasts along a depth profile. The profile will reveal the time-integrated concentrations from the different interaction pathways as the rock is advected toward the surface due to erosion. The exponential decrease in concentration will trend toward zero with depth if there is no inheritance. However, if C_{inh} is nonzero, the concentration versus depth curve will be asymptotic along the depth axis. The offset corresponds to the C_{inh} and can be subtracted from the measured concentration to solve for erosion or exposure age. Hidy et al. (2010) showed that amalgamations of hundreds of thousands of sand clasts provide a more precise solution than dozens of pebbles (pebbles seem to work in rapidly eroding catchments, whereas many more sand grains are necessary to characterize the average C_{inh} where catchment erosion rate is low, and C_{inh} is high and more variable).

Burial dating

When rock or sediment is buried and effectively shielded from any secondary cosmic ray flux, the concentration of TCNs in the buried minerals will change according to their decay rate. The noble gases will remain constant (assuming no unaccounted diffusion) and radionuclides with faster decay rates will decrease faster. The change in the ratio of the concentration of two (or more) different TCNs in the same sample, as long as one is a radionuclide, depends on burial duration, erosion rate, and depth. Burial dating has been contributed to many different disciplines:

- Glaciology and paleoclimatology: burial of bedrock by one or more episodes of glacier cover (e.g., Nishiizumi et al., 1991)
- Anthropology and archaeology: sediment and associated human fossils that were shielded in caves (e.g., Shen et al., 2009)
- Geomorphology and paleontology: fluvial terraces and alluvial back to the Pliocene (e.g., Rybczynski et al., 2013)

Simple burial dating with two isotopes

In the simplest case of a surface that had build up over exposure time (t) interrupted by a single period of complete shielding from cosmic rays (t_b), the burial duration can be determined using two TCNs with different mean lives (τ) in the same sample:

$$t_b = -\frac{\tau_{\text{short}}\tau_{\text{long}}}{\tau_{\text{long}} - \tau_{\text{short}}} \ln\left(\frac{P_{\text{long}(t,z,\varepsilon)} C_{\text{short}}}{P_{\text{short}(t,z,\varepsilon)} C_{\text{long}}}\right)$$

where C is the measured concentration and $P_{(t,z,\varepsilon)}$ is the sum of the time-averaged production rate over the time of exposure for a given depth and erosion rate for the short- or long-lived isotope (Granger and Muzikar, 2001). In this simple scenario, such as burial of a lava by another thick lava, there $C_{inh} = 0$ atoms g^{-1} and $\varepsilon = 0$ cm a^{-1}. Even if the initial exposure duration is not known, the pre-burial and burial durations may be solved if the ratio of the two isotopes fall below the steady-state island in a ratio plot (e.g., $^{26}Al/^{10}Be$ vs. ^{10}Be, Figure 2), erosion is assumed negligible, and the surface or sediment had never experienced a previous burial (or storage) event. This method requires two isotope measurements in only one sample. It assumes that burial was complete and instantaneous; otherwise, production during partial exposure at varying depths with time will need to be considered.

Isochron burial dating

Balco and Rovey (2008) provided an isochron solution for the common instance where a surface or sediment has undergone previous burial episodes. In these cases, the initial ratio of the isotopes measured in a sample does not correspond to the concentration for the production ratio $\left(\frac{P_{\text{short}(t,z,\varepsilon)}}{P_{\text{long}(t,z,\varepsilon)}}\right)$. Instead, prior burial durations will cause the concentration ratio to be lower at the beginning of the last burial episode. If ignored, the calculated burial duration will overestimate the burial age. By using an isochron approach (Figure 3), the concentration ratio prior to the last burial episode does not need to be known. The isochron approach requires that multiple samples are collected in the buried rock or sediment and that the concentrations of the TCN in each sample are different but that the ratio of the two TCN samples is the same. One option is to collect samples within a short (<1 m) depth profile interval below the burial contact. In this case the concentration for each TCN will diminish with depth if the buried minerals were exposed prior to burial. The greater the pre-burial exposure time, the greater the differences in concentration in the samples. However, the ratio of two spallogenic nuclides will be approximately constant over this short and shallow interval. For instance, on a $^{26}Al/^{10}Be$ isochron plot, the initial slope will be close to the production ratio (~6.75). During burial, the isotopic ratios will decrease at a rate proportional to their concentration, so the slope of their concentrations will decrease. The slope is proportional to the burial duration. In instances where exposure prior to burial was short (e.g., if eruption recurrence intervals were short) or there is no evidence of a paleosol because of significant erosion prior to burial, there are other options for obtaining multiple samples with different concentrations. For instance, there is a well-documented grain size dependency on concentration in sediments where deep-seated landsliding has occurred (Brown et al., 1995), so ^{26}Al and ^{10}Be concentrations in different grain size fractions from a single sample may be sufficiently distinct to define a ^{26}Al versus ^{10}Be slope.

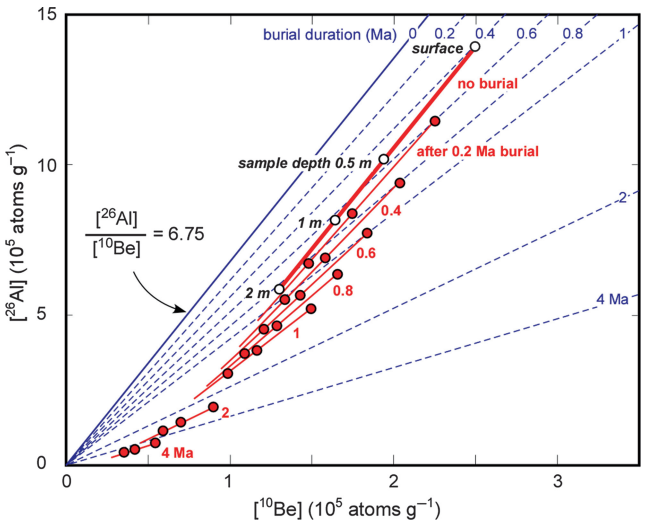

Terrestrial Cosmogenic Nuclide Dating, Figure 3 Concept of TCN burial isochron dating (Balco and Rovey, 2008), illustrated using a [^{26}Al]-[^{10}Be] plot. The ratio of samples collected from a continuously exposed soil (never buried) will plot on the *solid blue curve* depending on depth and exposure duration. *Blue dashed curves* represent sediment in a paleosol that was buried once (continuously) for the indicated duration. *Red curves* are defined by samples collected at different depths in sediment that had previously experienced burial and was redeposited and weathered in the modern paleosol. The initial ratios of the red samples in the paleosol would be less than the production ratio of the isotope pair (6.75 in the case of ^{26}Al/^{10}Be). The slope and position of the isochrons solve for initial ratio and burial duration simultaneously.

In the instance that multiple burial events have occurred, such as on a glaciated summit, different approaches have been used to constrain the possible burial history. The approaches use a combination of burial dating with two or more TCNs and an independent record of glaciation, such as an ice volume time series from a marine or ice sheet record. A recent approach reported by Margreth et al. (submitted) used the ratio of two radionuclides in two nearby surfaces, but one has been more recently plucked than the other. Considering periodic burial by ice, and even subaerial and episodic subglacial erosion, the concentrations and ratios help constrain the long-term (millions of years) fraction of ice-free time.

TCN applications: erosion rates

While erosion can contribute significantly to the uncertainty of exposure ages, the dependence of concentration on erosion increases the value of the TCN method. The TCN method can provide a direct estimate for erosion rate of local surfaces to large catchments. Erosion rates on bedrock surfaces have provided a means to establish background rates for comparison with recent erosion rates during the Anthropocene, or longer-term rates determined by thermochronology, or relief generation from the difference between valley and summit erosion rates.

In most applications of TCN erosion rate analysis, the overriding assumption is that the erosion was continuous and constant over the entire exposure duration. A single concentration in one sample on a surface constrains erosion (Eq. 5) if the radionuclide has reached its saturation concentration C^*. Saturation can be achieved more easily by using a short-lived isotope (e.g., ^{14}C) on a rapidly eroding surface (e.g., a sloped surface on a sediment, Figure 1). If the objective is to obtain an estimate of erosion over a longer time period than recorded by a short-lived TCN, but the C^* for the longer-lived isotopes has not been attained, then the erosion rate determined from Eq. 5 will be an estimate of the maximum erosion rate permitted to achieve the measured concentration. Multiple nuclides measured in one sample can provide the exposure duration and erosion rate of that surface (e.g., Nishiizumi et al., 1991; Phillips et al., 1997).

It is also possible to apply Eq. 5 to estimate the denudation rate of an entire catchment. While the approach was first conducted using meteoric ^{10}Be absorbed on regolith delivered to streams (Brown et al., 1988), the method now uses the lower concentrations of in situ TCN in the same sediments (Brown et al., 1995; Granger et al., 1996). The approach assumes that at each location in a catchment, the concentration at the surface has reached saturation. However, instead of tagging the C^* and therefore ε at every surface in the basin, the hillslope processes and streams will deliver a flux of sediment that is scaled with the erosion rate of the upstream slopes. Thus, one sample of modern stream sediment provides an estimate of basin-average erosion rate for all catchment surfaces above that point. A basin TCN production rate can be calculated by taking the average of production rates for each pixel in the DEM; scaled for latitude, longitude, and elevation; and adjusted for topographic shielding, vegetation, and other factors. The basin-average erosion rate method relies on the constant delivery of sediment from all surfaces in the catchment and assumes a homogeneous distribution of the mineral of choice. Special approaches are required if some areas of the catchment are not eroding or have no target mineral of the selected grain size. The duration over which the erosion rate is applicable depends on the radionuclide decay rate and the erosion rate of the catchment (faster rates reduce the averaging time).

It is also possible to determine the paleo-erosion rate of a basin (Schaller et al., 2002; Hidy et al., 2014). Instead of using modern sediment, it is necessary to sample sediment stored in the catchment that was deposited at the time of interest. In order to obtain the average depositional concentration (C_{dep}) for a given time in the past, we determine the inherited concentration (C_{inh}, e.g., with a depth profile) and compensate for the concentration lost to decay over the time since deposition. Time since deposition may be determined with TCN methods or independently with a different dating method. The method assumes that any changes in catchment elevation, relief, area, or target mineral abundance with time are negligible or known.

Uncertainty and assumptions of TCN exposure ages and erosion rates

Arguably more than any other dating method described in this encyclopedia, the TCN dating method is more sensitive to sample and environmental context. For this reason, it is challenging to establish a rigorous analysis of total uncertainty in an exposure age, burial age, or erosion rate (Borchers et al., submitted). There is no consensus on whether or not 1σ or 2σ uncertainties shall be reported. In some instances involving Monte Carlo approaches, the only fits obtainable are at the 3σ level and that error is not reduced to a lower confidence level.

Internal random errors affect the precision of the measurement. These include (i) AMS or MS precision (typically based on a Poisson distribution, averaging 2–3 % 1σ), (ii) uncertainty in the spike or carrier concentration (generally better than 2 % 1σ), and (iii) contribution to the measurement of the process blank, calculated by considering what fraction of the sample measurement was contributed by the process (usually <1 % except for very low-level measurements). As ^{36}Cl requires elemental analysis of potential target elements, and thermal-neutron absorbers and producers, the uncertainty in ICP, ICP.MS, or XRF measurements is also incorporated.

The principal external error is uncertainty in the scaled and time-averaged production rate. Balco et al., 2008 recommended approximately 10 % 1σ uncertainty, and it is unclear if the production rate uncertainty has improved for each TCN since then.

Most publications do not consider the other sources of error that relate to the various environmental conditions that affect production rate or add complexity to the exposure and burial history. In the newest CRONUS-Earth online calculator, uncertainties for all of the required input parameters are requested, including uncertainty in the shielding factors for snow, vegetation, geometry, topography, and effective attenuation lengths. Hidy et al. (2010) also incorporated the stochastically or normally distributed uncertainties in bulk density and inheritance in evaluating error for depth profile ages and erosion rates. Still typically non-quantified are errors associated with surface uplift, erosion, episodic erosion, burial and aggradation, exhumation, mixing, and other factors.

Numerous comparisons of TCN surface exposure ages of rock surfaces and sediments and other dating methods have been published, and summaries of recent interlaboratory comparisons and duplication measurements have been reported in Jull et al. (2013) and Phillips et al. (2014 submitted). These include alluvial depositional ages against OSL in the same section, erratic boulder exposure ages against calibrated radiocarbon ages, and exposure ages on lava dated with ^{40}Ar/^{39}Ar.

Assumptions common to many TCN dating applications

- The TCN production rate is known for a given production pathway. This is the major source of uncertainty in the dating method. The production rate varies as a function of (i) temporal and spatial variations in dipole and non-dipole magnetic field controls on the GCR flux to the atmosphere (Lal, 1991; Lifton et al., 2014), (ii) temporal and spatial variations in atmospheric shielding of GCR and secondaries (Lal and Peters, 1967; Stone, 2000; Staiger et al., 2007), and (iii) depth below the surface because of attenuation of the cosmic ray flux through different interactions that depend on the energy spectra and type of secondary and the chemistry of the mineral matter.
- All cosmogenic, radiogenic, and nucleogenic pathways are recognized. For TCN exposure dating the primary cosmogenic production pathways are spallation, capture, and muonic interactions (Lal, 1991; Gosse and Phillips, 2001).
- Any initial TCN concentration prior to the exposure of interest is negligible or can be determined independently, e.g., with depth profiles through sediment (Anderson et al., 1996).
- The cosmic ray flux is constant. The uncertainty in this assumption has not been well established (e.g., Wieler et al., 2013).
- TCN concentrations are measured accurately. While the majority of modern measurements with noble gas mass spectrometers or accelerator mass spectrometers (AMS) average 2–4 % 1σ precision for some TCN (Vermeesch et al., 2012; Jull et al., 2013), the actual range of internal measurement precisions evaluated by duplicates and interlaboratory comparisons can be larger. Low TCN concentrations due to small sample mass, low production rate, short exposure time, or long burial time will increase uncertainty because of counting statistics (Poisson distribution), the uncertainty in blank correction (by nature, the process blanks will have poor counting statistics), spectrometry detection limits, and, in the case of AMS, normalization with standards with TCN abundances that are more than two orders of magnitude greater that the low-level samples.
- No unaccounted surface processes have influenced the exposure or erosion history of the minerals being dated. For instance, there is negligible or known effects of (i) erosion of the rock surface (Gillespie and Bierman, 1995): (ii) shielding and the moderating effects of snow (Gosse and Phillips, 2001; Zweck et al., 2013; Delunel et al., 2014), soil moisture (Dunai et al., 2014), ice, or forests and vegetation (Plug et al., 2007); (iii) exhumation (Putkonen and Swanson, 2003); and (iv) movement of the dated material by tectonics, isostasy, mixing, or rotation during exposure.

Bibliography

Anderson, R. S., Repka, J. L., and Dick, G. S., 1996. Explicit treatment of inheritance in dating depositional surfaces using in situ ^{10}Be and ^{26}Al. *Geology*, **24**(1), 47–51.

Argento, D. C., Reedy, R. C., and Stone, J. O., 2013. Modeling the Earth's cosmic radiation. *Nuclear Instruments and Methods in Physics Research Section B*, **294**, 464–469.

Balco, G., and Rovey, C. W., 2008. An isochron method for cosmogenic-nuclide dating of buried soils and sediments. *American Journal of Science*, **308**(10), 1083–1114.

Balco, G., Stone, J. O., Lifton, N. A., and Dunai, T. J., 2008. A complete and easily accessible means of calculating surface exposure ages or erosion rates from ^{10}Be and ^{26}Al measurements. *Quaternary Geochronology*, **3**(3), 174–195.

Beer, J., Bonani, G., Hofmann, H. J., Suter, M., Synal, A., Wölfli, W., Oeschger, H., Siegenthaler, U., and Finkel, R. C., 1987. ^{10}Be measurements on polar ice: comparison of Arctic and Antarctic records. *Nuclear Instruments and Methods in Physics Research Section B*, **29**(1), 203–206.

Borchers, B., Marrero, S., Balco, G., Caffee, M., Goehring, B., Gosse, J., Lifton, N., Nishiizumi, K., Phillips, F., Schaefer, J., Stone, J.O.H., (submitted). Geological calibration of spallation production rates for terrestrial cosmogenic nuclides in the CRONUS-Earth Project. *Quaternary Geochronology.*

Brown, L., Klein, J., Middleton, R., Sacks, I. S., and Tera, F., 1982. 10Be in island-arc volcanoes and implications for subduction. *Nature*, **299**(5885), 718–720.

Brown, L., Pavich, M. J., Hickman, R. E., Klein, J., and Middleton, R., 1988. Erosion of the eastern United States observed with ^{10}Be. *Earth Surface Processes and Landforms*, **13**(5), 441–457.

Brown, E. T., Stallard, R. F., Larsen, M. C., Raisbeck, G. M., and Yiou, F., 1995. Denudation rates determined from the accumulation of in situ-produced ^{10}Be in the Luquillo experimental forest, Puerto Rico. *Earth and Planetary Science Letters*, **129**(1), 193–202.

Brown, E. T., Bendick, R., Bourles, D. L., Gaur, V., Molnar, P., Raisbeck, G. M., and Yiou, F., 2002. Slip rates of the Karakoram fault, Ladakh, India, determined using cosmic ray exposure dating of debris flows and moraines. *Journal of Geophysical Research Solid Earth (1978–2012)*, **107**(B9), ESE-7.

Craig, H., and Poreda, R. J., 1986. Cosmogenic ^{3}He in terrestrial rocks: the summit lavas of Maui. *Proceedings of the National Academy of Sciences*, **83**(7), 1970–1974.

Davis, R., and Schaeffer, O. A., 1955. Chlorine-36 in nature. *Annals of the New York Academy of Sciences*, **62**(5), 107–121.

Delunel, R., Bourlès, D. L., van der Beek, P. A., Schlunegger, F., Leya, I., Masarik, J., and Paquet, E., 2014. Snow shielding factors for cosmogenic nuclide dating inferred from long-term neutron detector monitoring. *Quaternary Geochronology*, **24**, 16–26.

Drozd, R. J., Hohenberg, C. M., Morgan, C. J., and Ralston, C. E., 1974. Cosmic-ray exposure history at the Apollo 16 and other lunar sites: lunar surface dynamics. *Geochimica et Cosmochimica Acta*, **38**(10), 1625–1642.

Dunai, T. J., 2010. *Cosmogenic Nuclides: Principles, Concepts and Applications in the Earth Surface Sciences*. Cambridge: Cambridge University Press.

Dunai, T. J., López, G. A. G., and Juez-Larré, J., 2005. Oligocene–Miocene age of aridity in the Atacama Desert revealed by exposure dating of erosion-sensitive landforms. *Geology*, **33**(4), 321–324.

Dunai, T. J., Binnie, S. A., Hein, A. S., and Paling, S. M., 2014. The effects of a hydrogen-rich ground cover on cosmogenic thermal neutrons: implications for exposure dating. *Quaternary Geochronology*, **22**, 183–191.

Eugster, O., Herzog, G. F., Marti, K., and Caffee, M. W., 2006. Irradiation records, cosmic-ray exposure ages, and transfer times of meteorites. *Meteorites and the early solar system II*, **1**, 829–851.

Farley, K. A., Malespin, C., Mahaffy, P., Grotzinger, J. P., Vasconcelos, P. M., Milliken, R. E., Floyd, M., et al., 2014. In situ radiometric and exposure age dating of the Martian surface. *Science*, **343**(6169), 1247166.

Gilichinsky, D. A., Nolte, E., Basilyan, A. E., Beer, J., Blinov, A. V., Lazarev, V. E., Tumskoy, V. E., et al., 2007. Dating of syngenetic ice wedges in permafrost with ^{36}Cl. *Quaternary Science Reviews*, **26**(11), 1547–1556.

Gillespie, A. R., and Bierman, P. R., 1995. Precision of terrestrial exposure ages and erosion rates estimated from analysis of cosmogenic isotopes produced in situ. *Journal of Geophysical Research Solid Earth (1978–2012)*, **100**(B12), 24637–24649.

Gosse, J. C. (2012). Terrestrial cosmogenic nuclide techniques for assessing exposure history of surfaces and sediments in active tectonic regions. *Tectonics of Sedimentary Basins: Recent Advances*, 63–79.

Gosse, J. C., and Phillips, F. M., 2001. Terrestrial in situ cosmogenic nuclides: theory and application. *Quaternary Science Reviews*, **20**(14), 1475–1560.

Granger, D. E., and Muzikar, P. F., 2001. Dating sediment burial with in situ-produced cosmogenic nuclides: theory, techniques, and limitations. *Earth and Planetary Science Letters*, **188**(1), 269–281.

Granger, D. E., Kirchner, J. W., and Finkel, R., 1996. Spatially averaged long-term erosion rates measured from in situ-produced cosmogenic nuclides in alluvial sediment. *The Journal of Geology*, **104**, 249–257.

Granger, D. E., Lifton, N. A., and Willenbring, J. K., 2013. A cosmic trip: 25 years of cosmogenic nuclides in geology. *Geological Society of America Bulletin*, **125**(9–10), 1379–1402.

Grosse, A. V., 1934. An unknown radioactivity. *Journal of the American Chemical Society*, **56**(9), 1922–1924.

Hampel, W., Takagi, J., Sakamoto, K., and Tanaka, S., 1975. Measurement of muon-induced ^{26}Al in terrestrial silicate rock. *Journal of Geophysical Research*, **80**(26), 3757–3760.

Heisinger, B., Lal, D., Jull, A. J. T., Kubik, P., Ivy-Ochs, S., Knie, K., and Nolte, E., 2002a. Production of selected cosmogenic radionuclides by muons: 2. Capture of negative muons. *Earth and Planetary Science Letters*, **200**(3), 357–369.

Heisinger, B., Lal, D., Jull, A. J. T., Kubik, P., Ivy-Ochs, S., Neumaier, S., Knie, K., Lazarev, V., and Nolte, E., 2002b. Production of selected cosmogenic radionuclides by muons: 1. Fast muons. *Earth and Planetary Science Letters*, **200**(3), 345–355.

Herzog, G. F., 2010. Cosmic-ray exposure ages of meteorites. *Treatise of Geochemistry*, **1**, 1–36.

Hess, V. F., 1912. Penetrating radiation in seven free balloon flights. *Zeitschrift fuer Physik*, **13**, 1084.

Hidy, A. J., Gosse, J. C., Pederson, J. L., Mattern, J. P., Finkel, R. C., et al., 2010. A geologically constrained Monte Carlo approach to modeling exposure ages from profiles of cosmogenic nuclides: an example from Lees Ferry, Arizona. *Geochemistry, Geophysics, Geosystems*, **11**(9), 1–18.

Hidy, A. J., Gosse, J. C., Blum, M. D., and Gibling, M. R., 2014. Glacial–interglacial variation in denudation rates from interior Texas, USA, established with cosmogenic nuclides. *Earth and Planetary Science Letters*, **390**, 209–221.

Jull, A. J., Scott, E. M., and Bierman, P., 2013. The CRONUS-Earth inter-comparison for cosmogenic isotope analysis. *Quaternary Geochronology.*

Klein, J., Giegengack, R., Middleton, R., Sharma, P., Underwood, J. R., and Weeks, R. A., 1986. Revealing histories of exposure using in situ produced ^{26}Al and ^{10}Be in Libyan desert glass. *Radiocarbon*, **28**(2A), 547–555.

Kober, F., Alfimov, V., Ivy-Ochs, S., Kubik, P. W., and Wieler, R., 2011. The cosmogenic ^{21}Ne production rate in quartz evaluated on a large set of existing ^{21}Ne–^{10}Be data. *Earth and Planetary Science Letters*, **302**(1), 163–171.

Kurz, M. D., 1986. In situ production of terrestrial cosmogenic helium and some applications to geochronology. *Geochimica et Cosmochimica Acta*, **50**(12), 2855–2862.

Lal, D., 1991. Cosmic ray labeling of erosion surfaces: in situ nuclide production rates and erosion models. *Earth and Planetary Science Letters*, **104**(2), 424–439.

Lal, D., and Peters, B., 1967. Cosmic ray produced radioactivity on the earth. In *Kosmische Strahlung II/Cosmic Rays II*. Berlin/Heidelberg: Springer, pp. 551–612.
Lifton, N., Sato, T., and Dunai, T. J., 2014. Scaling in situ cosmogenic nuclide production rates using analytical approximations to atmospheric cosmic-ray fluxes. *Earth and Planetary Science Letters*, **386**, 149–160.
Margreth, A., Gosse, J., Dyke, A., Plug, L., (submitted). Episodic erosion rates on high latitude glaciated uplands. *Quaternary Science Reviews*.
Masarik, J., and Reedy, R. C., 1995. Terrestrial cosmogenic-nuclide production systematics calculated from numerical simulations. *Earth and Planetary Science Letters*, **136**(3), 381–395.
Mercader, J., Gosse, J. C., Bennett, T., Hidy, A. J., and Rood, D. H., 2012. Cosmogenic nuclide age constraints on middle stone age lithics from Niassa, Mozambique. *Quaternary Science Reviews*, **47**, 116–130.
Morris, J. D., Gosse, J., Brachfeld, S., and Tera, F., 2002. Cosmogenic Be-10 and the solid Earth: studies in geomagnetism, subduction zone processes, and active tectonics. *Reviews in Mineralogy and Geochemistry*, **50**(1), 207–270.
Nishiizumi, K., Lal, D., Klein, J., Middleton, R., and Arnold, J. R., 1986. Production of ^{10}Be and ^{26}Al by cosmic rays in terrestrial quartz in situ and implications for erosion rates. *Nature*, **319**, 134–136.
Nishiizumi, K., Kohl, C. P., Arnold, J. R., Klein, J., Fink, D., and Middleton, R., 1991. Cosmic ray produced ^{10}Be and ^{26}Al in Antarctic rocks: exposure and erosion history. *Earth and Planetary Science Letters*, **104**(2), 440–454.
Olive, K.A., et al., (Particle Data Group), 2014. Review of particle physics. *Chinese Physics*, **C38**, 090001.
Phillips, F. M., and Plummer, M. A., 1996. CHLOE; a program for interpreting in-situ cosmogenic nuclide data for surface exposure dating and erosion studies. *Radiocarbon*, **38**(1), 98–99.
Phillips, F. M., Leavy, B. D., Jannik, N. O., Elmore, D., and Kubik, P. W., 1986. The accumulation of cosmogenic chlorine-36 in rocks: a method for surface exposure dating. *Science*, **231**(4733), 41–43.
Phillips, F. M., Zreda, M. G., Gosse, J. C., Klein, J., Evenson, E. B., Hall, R. D., Chadwick, O. A., and Sharma, P., 1997. Cosmogenic ^{36}Cl and ^{10}Be ages of quaternary glacial and fluvial deposits of the Wind River Range, Wyoming. *Geological Society of America Bulletin*, **109**(11), 1453–1463.
Phillips, F.M., et al., (2014, submitted). The CRONUS-Earth project: a synthesis. *Quaternary Geochronology.*
Plug, L. J., Gosse, J. C., McIntosh, J. J., and Bigley, R., 2007. Attenuation of cosmic ray flux in temperate forest. *Journal of Geophysical Research Earth Surface (2003–2012)*, **112**(F2), 1–9.
Putkonen, J., and Swanson, T., 2003. Accuracy of cosmogenic ages for moraines. *Quaternary Research*, **59**(2), 255–261.
Reedy, R. C., Arnold, J. R., and Lal, D., 1983. Cosmic-ray record in solar system matter. *Science*, **219**(4581), 127–135.
Rybczynski, N., Gosse, J. C., Harington, C. R., Wogelius, R. A., Hidy, A. J., and Buckley, M., 2013. Mid-Pliocene warm-period deposits in the high Arctic yield insight into camel evolution. *Nature Communications*, **4**, 1550.
Schaller, M., Von Blanckenburg, F., Veldkamp, A., Tebbens, L. A., Hovius, N., and Kubik, P. W., 2002. A 30 000 yr record of erosion rates from cosmogenic ^{10}Be in middle European river terraces. *Earth and Planetary Science Letters*, **204**(1), 307–320.
Shen, G., Gao, X., Gao, B., and Granger, D. E., 2009. Age of Zhoukoudian Homo erectus determined with ^{26}Al/^{10}Be burial dating. *Nature*, **458**(7235), 198–200.
Staiger, J., Gosse, J., Toracinta, R., Oglesby, B., Fastook, J., and Johnson, J. V., 2007. Atmospheric scaling of cosmogenic nuclide production: climate effect. *Journal of Geophysical Research Solid Earth (1978–2012)*, **112**(B2), 1–12.
Stone, J. O., 2000. Air pressure and cosmogenic isotope production. *Journal of Geophysical Research Solid Earth (1978–2012)*, **105**(B10), 23753–23759.
Vermeesch, P., 2007. CosmoCalc: an excel add-in for cosmogenic nuclide calculations. *Geochemistry, Geophysics, Geosystems*, **8**(8), 1–14.
Vermeesch, P., Balco, G., Blard, P. H., Dunai, T. J., Kober, F., Niedermann, S., Zimmermann, L., et al., 2012. Interlaboratory comparison of cosmogenic ^{21}Ne in quartz. *Quaternary Geochronology.*
Wieler, R., Beer, J., and Leya, I., 2013. The galactic cosmic ray intensity over the past 10^6–10^9 years as recorded by cosmogenic nuclides in meteorites and terrestrial samples. *Space Science Reviews*, **176**(1–4), 351–363.
Zweck, C., Zreda, M., and Desilets, D., 2013. Snow shielding factors for cosmogenic nuclide dating inferred from Monte Carlo neutron transport simulations. *Earth and Planetary Science Letters*, **379**, 64–71.

Cross-references

Accelerator Mass Spectrometry
Glacial Landscape (Cosmogenic Nuclide)
Luminescence, Rock Surfaces
Meteoric ^{10}Be
Meteorites (^{36}Cl)
Noble Gas Mass Spectrometer
Radiocarbon Dating

THERMAL IONIZATION MASS SPECTROMETER (TIMS)

Roland Mundil
Berkeley Geochronology Center, Berkeley, CA, USA

Definition

A thermal ionization mass spectrometer (TIMS) consists of (1) an ion source (here a solid source), (2) a magnet (analyzer) that splits the ions depending on their mass to charge ratio (momentum filter), and (3) one or multiple collectors that measure the magnitude of the ion beams such that isotopic ratios of a given element can be computed (Nier-type spectrometer, Nier, 1940).

Prior to analysis, a solution containing the purified sample is loaded on a metal filament (Re, Ta, Pl, or W) and dried down. In the evacuated source, ions are generated using the process of surface ionization by thermally heating the filament to ca. 1,200–1,800 ºC. In a single-filament configuration, ions are directly emitted from the loaded sample; in a double- or triple-filament configuration, the sample is loaded on one or both of the side filaments where volatilization takes place followed by ionization using the center filament that is heated to a significantly higher temperature. Depending on the element, the use of various emitter substances can be used to enhance and stabilize the ionization. Most elements are analyzed as positive ions and some as negative ions (e.g., OsO_3^-, WO_3^-). Ionization efficiency depends on

http://www.springer.com/978-94-007-6303-6

Encyclopedia of Scientific Dating Methods
Rink, W.J.; Thompson, J.W. (Eds.)
2015, XXIX, 978 p. 375 illus., 260 illus. in color.,
Hardcover
ISBN: 978-94-007-6303-6